Research in Astronomy and Astrophysics, 24:065023 (7pp), 2024 June https://doi.org/10.1088/1674-4527/ad47dd

V0405 Dra: A New Deep and Low Mass Ratio Contact Binary with Extremely Fast Decrease in the Orbital Period

Chao-Yue Li[1], Lin-Qiao Jiang[1,2,3], Jie Zheng[4], Yi-Man Liu[1], Xiao-Yu Long[1], Min Sun[1], Han-Lu Zhang[1], and Xiao-Man Tian[5]
[1] School of Science, Leshan Normal University, Leshan 614000, China; jianglinqiao11@163.com
[2] Center for Applied Optics Research, Leshan Normal University, Leshan 614000, China
[3] Key Laboratory of Detection and Application of Space Effect in Southwest Sichuan, Leshan 614000, China
[4] CAS Key Laboratory of Optical Astronomy, National Astronomical Observatories, Chinese Academy of Sciences, Beijing 100101, China
[5] School of Aeronautics, Shandong Jiaotong University, Jinan 250000, China
Received 2024 March 20; revised 2024 April 23; accepted 2024 April 29; published 2024 June 4

Abstract

V0405 Dra is a W UMa-type binary star. Based on the TESS data, we have conducted an orbital period study and performed a light curve analysis for the system. The orbital period study reveals that the $O-C$ curve for V0405 Dra exhibits secular decrease at an extremely high rate of $dP/dt = -2.71 \times 10^{-6}$ day year^{-1}, along with periodic variations characterized by an amplitude of $A_3 = 0.0032$ day and a period of $P_3 = 1.413$ years. The orbital periodic change is possibly due to the light-travel time effect resulting from an additional third body in the system, for which we estimate a minimum mass of $M_3 = 0.77M_{\odot}$. By employing the 2013 version of the Wilson-Devinney (W-D) method to synthesize a light curve, we derived photometric solutions indicating that V0405 Dra is a new deep ($f = 68.7\%$) and low-mass ratio ($q = 0.175$) contact binary. The fast decrease in its orbital period is likely caused by mass transfer from the more massive primary star to the less massive secondary star, or due to angular momentum loss. With further mass transfer and loss of angular momentum, the binary will gradually evolve into a tighter contact configuration, eventually leading to a merger into a single star, following the evolutionary paths suggested for such deep and low mass ratio contact binaries.

Key words: (stars:) binaries (including multiple): close – (stars:) binaries: eclipsing – stars: individual (V0405 Dra)

1. Introduction

W Ursae Majoris (W UMa)-type contact binaries generally comprise two late-type stars (Kopal 1955). Due to their short orbital periods, typically ranging from 0.2 to 1.5 days, they are the most commonly observed type of eclipsing binary systems (Geske et al. 2006). Researches indicate the close proximity of the two stars in a contact binary, under the combined influence of strong gravity and rotation (synchronization of rotation and revolution), causes the stars in the system to elongate along the line joining their centers of mass and become flattened along their rotational axes, resulting in a dumbbell-shaped structure of the contact binary (Kopal 1978). This structure causes the contact binary to exhibit eclipse features when the orbital inclination angle i exceeds 34 degrees (Kopal 1978), and leads to continuous changes in brightness between the eclipses. Based on the light curve characteristics, Binnendijk (1970) classified W UMa-type contact binaries into A- and W-subtypes. Orbital period variability in such systems typically follows one or two patterns, including long-term increase or decrease, cyclic oscillation (Kreiner et al. 2001), and irregular changes. These variations could arise from processes like mass and angular momentum transfer or loss within or outside the system, apsidal motion, the light-travel time effect (Irwin 1952), cyclic magnetic activity (Applegate 1992), and other physical mechanisms (Li & Zhang 2006; Yuan & Qian 2007). Studying the orbital period variations of W UMa-type contact systems can offer significant insights into the dynamics of binary stars, enhance our knowledge of stellar structure and evolution under various conditions, and shed light on certain astrophysical properties.

Contact binaries with a mass ratio less than 0.25 and a contact degree greater than 50% are defined as deep and low-mass-ratio contact binaries (hereafter DLMRCBs) (Qian et al. 2005; Zhu et al. 2011). They could offer an excellent opportunity to study scenarios of stellar mergers (Stepien 2006). By examining the long-term period changes in DLMRCBs, Qian et al. (2006) proposed two potential evolutionary scenarios by which DLMRCBs can evolve into Blue Straggler/FK Com-type stars: systems with a decreasing period will experience a contraction of the inner and outer critical Roche lobes, and this contraction would enhance the degree of contact configuration; once the photospheric surface reaches the outer critical lobe, these systems will merge rapidly due to dynamic instability (Meng et al. 2023). While systems with an increasing period are undergoing the mass transfer from the less massive component to the more massive one, such a process could result in the decrease of mass ratio and the

Table 1
The Observation Log of V0405 Dra by TESS

Sector	Observation Start Time	Observation End Time	Time Span (BJD)	Exposure Time (s)
sector14	2019.07.18	2019.08.14	2458683-2458710	120
sector15	2019.08.15	2019.09.10	2458711-2458737	120
sector22	2020.02.19	2020.03.17	2458899-2458926	120
sector25	2020.05.14	2020.06.08	2458983-2459009	120
sector26	2020.06.09	2020.07.04	2459010-2459035	120
sector40	2021.06.25	2021.07.23	2459390-2459418	120
sector41	2021.07.24	2021.08.20	2459419-2459446	120
sector52	2022.05.19	2022.06.12	2459718-2459743	120
sector53	2022.06.13	2022.07.08	2459743-2459768	120
sector54	2022.07.09	2022.08.04	2459769-2459796	120
sector55	2022.08.05	2022.09.01	2459797-2459824	120
sector58	2022.10.29	2022.11.26	2459882-2459910	120
sector59	2022.11.26	2022.12.23	2459910-2459936	120

increase of $J_{\rm spin}/J_{\rm orb}$. Only if they meet the criteria of $J_{\rm orb} < 3J_{\rm spin}$ and are still in contact configuration will they evolve into the rapid-rotating single stars (Yang et al. 2021). Therefore, DLMRCBs are identified at a late stage in the evolutionary process of contact binaries and are regarded as the progenitors of merging stars (Zhou et al. 2016; Sarotsakulchai et al. 2018).

V0405 Dra was first classified as an EW-subtype contact binary based on observations from ROTSE-I (Akerlof et al. 2000). Terrell et al. (2012) reported a period of $0\overset{\circ}{.}41303100$ as one of the 606 W UMa binary star systems observed during at least three photometric nights at a robotic observatory in southern Arizona. The first orbital period change analysis of V0405 Dra was conducted by Pyatnytskyy & Andronov (2022). Utilizing survey data, literature sources, and their own observations, they determined a period increase rate of $2.72(\pm 0.03) \times 10^{-6}\ \mathrm{yr}^{-1}$. In addition to the long-term period increase, analysis of TESS data reveals evidence of cyclic variations. They assessed the period of the cyclic variations to be 1.473 yr, with a semi-amplitude of 0.002 day. Until now, there has been no publication related to its light curve solution. Fortunately, TESS offers high-precision photometric data owing to its continuous and uninterrupted observations, as well as its high temporal resolution (Ricker et al. 2015), enabling the study of continuous variations in V0405 Dra. Therefore, we have decided to conduct a light curve study on V0405 Dra using TESS data. The second part of this paper presents the light curve of V0405 Dra captured by TESS. Parts three and four discuss the analysis of orbital period changes and photometric analysis respectively, followed by a final discussion.

2. TESS Photometric Data

While TESS's primary mission is focused on the search for exoplanets, it also provides a wealth of high-precision photometric data. These data open up extensive opportunities for research into variable stars. Coincidentally, V0405 Dra is included in its observation list. TESS has provided photometric data for 13 sectors (sector14, sector15, sector22, sector25, sector26, sector40, sector41, sector52, sector53, sector54, sector55, sector58, and sector59) of V0405 Dra, with each sector having an exposure time of 2 minutes. Detailed observational information about the sectors can be found in Table 1. We adopt the light curves of SAP_FLUX (simple aperture photometry data) downloaded from the Mikulski Archive for Space Telescopes (MAST)[6] database. We transform all photometric data into normalized flux using the Lightkurve and pltgui package in Python (Lightkurve Collaboration et al. 2018). The normalized light curves across all sectors are depicted in the upper part of Figure 1. It is observable that the light curve shape of V0405 Dra maintains symmetry and is stable throughout the time observed by TESS. We randomly selected a segment of the light curve for magnified display, as shown in the lower part of Figure 1.

3. Study of Orbital Period Changes

In contact binary systems, mass transfer and the presence of third bodies are relatively common phenomena (Duchêne & Kraus 2013; Qian et al. 2020). What is more interesting is the third bodies may be more massive than the the central binary system (Zhou & Soonthornthum 2019). The analysis of the orbital period can reveal the interactions within the binary or triple systems. In order to investigate the orbital period variations of V0405 Dra, we employ the least squares method to perform a quadratic fit on all the light curves observed by TESS. A total of 1584 instances of minimum light are obtained, as shown in Table 2. We utilize an initial period of $0\overset{d}{.}41303100$ (Terrell et al. 2012) to compute the $O - C$ values for all the light times of minimum, resulting in the following

[6] https://mast.stsci.edu/portal/Mashup/Clients/Mast/Portal.html

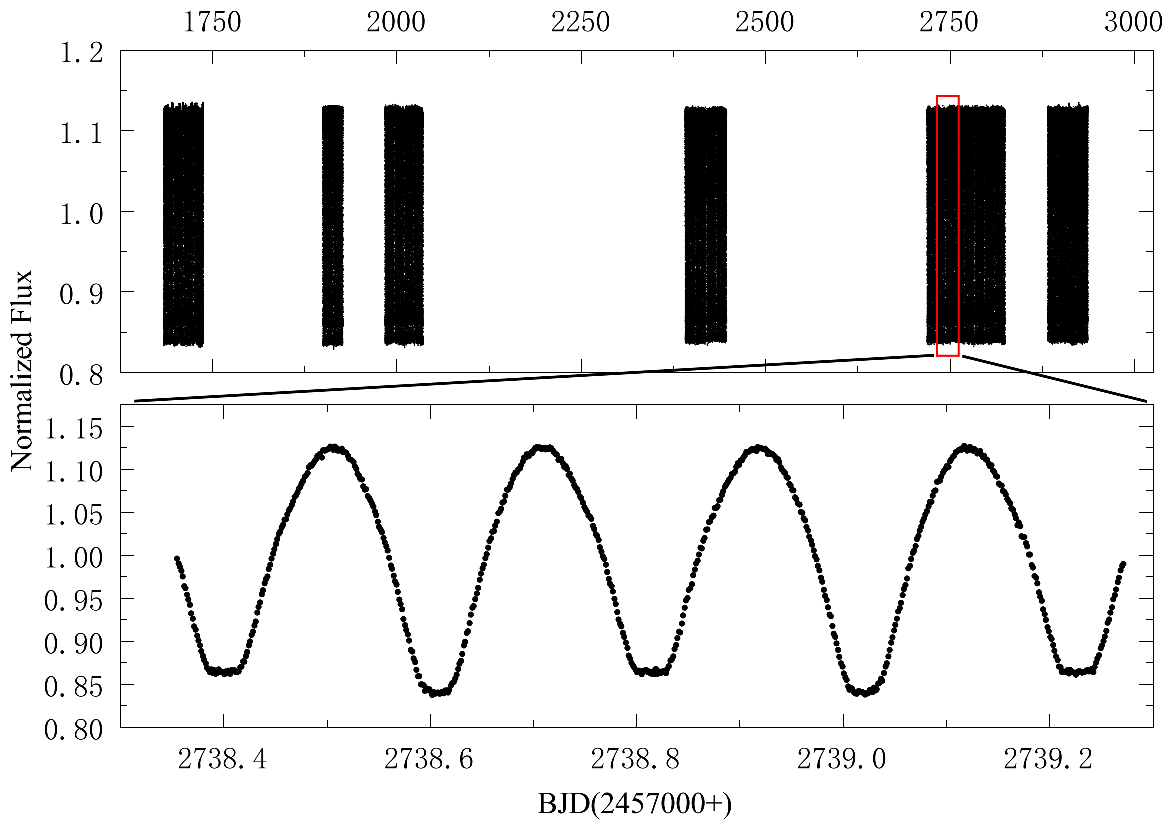

Figure 1. TESS photometric data of normalized flux.

Table 2
The Light Minimum Times of V0405 Dra

BJD	Error	E	$(O-C)_1$	$(O-C)_2$	Residuals	Min
2458683.677531	0.000267	0	0.001000	0.002280	0.000050	I
2458684.090832	0.000272	1	0.001251	0.002530	0.000290	I
2458684.503715	0.000256	2	0.001085	0.002350	0.000100	I
2458684.916849	0.000268	3	0.001169	0.002440	0.000170	I
2458685.330002	0.000267	4	0.001273	0.002530	0.000260	I
...	...	...	...	...	...	...
2459934.593308	0.000258	3028.5	−0.003573	−0.000770	−0.000090	II
2459935.006269	0.000256	3029.5	−0.003662	−0.000860	−0.000160	II
2459935.419347	0.000262	3030.5	−0.003633	−0.000820	−0.000120	II
2459935.832369	0.000261	3031.5	−0.003661	−0.000850	−0.000120	II
2459936.245425	0.000263	3032.5	−0.003654	−0.000830	−0.000100	II

new ephemeris formula

$$\begin{aligned} Min.I = BJD2458683.676531(86) \\ + 0^d.41304947(4) \times E. \end{aligned} \quad (1)$$

The $(O-C)_1$ values are calculated using the updated ephemeris formula (1), which are listed in Table 2 and depicted in the upper part of Figure 2. As illustrated in the figure, it is evident that the $(O-C)_1$ curve exhibits periodic oscillations, and there is an additional overall downward parabolic trend. Comparing our finding from $(O-C)_1$ with the research results of Pyatnytskyy & Andronov (2022), while both studies identify orbital periodic variations, the discrepancy arises in the absence of observed upward parabolic changes in $(O-C)_1$, indicating a long-term increase in the period. However, the cause of this discrepancy remains unclear. During the TESS observation period, the light curves exhibited completely symmetric and stable periodic variations. Therefore, we are inclined to believe

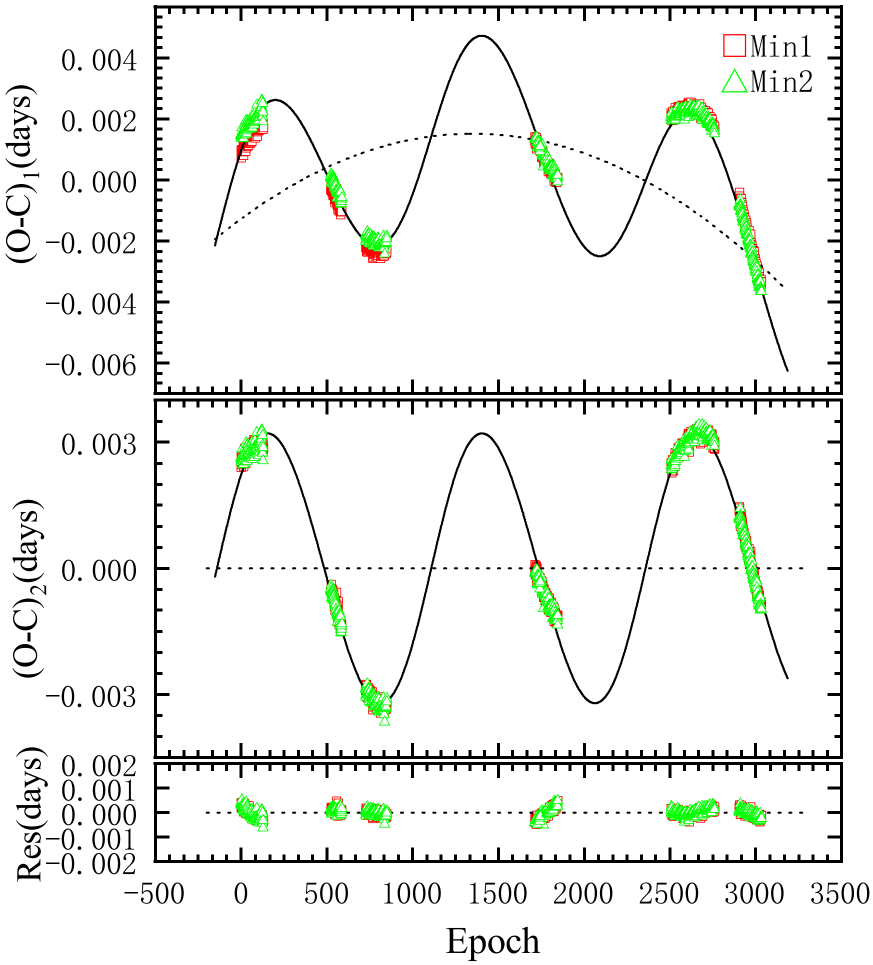

Figure 2. Upper part: $(O-C)_1$ values calculated by Equation (1). The solid and dotted lines are plotted using Equation (2); Middle part: $(O-C)_2$ diagram after the parabolic trend has been removed; Lower part: Residual diagram after eliminating all trends.

that the periodic variations are attributed to the light-travel time effect, which is induced by the presence of a third body. Hence, we employ the following equation to fit the $(O-C)_1$ curve

$$(O-C)_1 = \Delta T + \Delta P \times E + Q \times E^2 + A \times \left[\frac{1-e^2}{1+e\cos\upsilon}\sin(\upsilon+\omega) + e\sin\omega\right]. \quad (2)$$

In the equation, ΔT, ΔP and Q represent the correction of the initial epoch time, the correction of the orbital period and the changing rate of the orbital period. The final term represents the light-travel time effect (Irwin 1952), where $A = a_{12}\sin i/c$, P_3, e, ω and υ are the orbital parameters for the eclipsing pair around the mass center of the triple system. The fitted parameters and their uncertainties are simultaneously derived by the L-M algorithm (Yang 2009), which are tabulated in Table 3. The quadratic term in formula (2) suggests that the orbital period of V0405 Dra is decreasing at a rate of $dP/dt = -2.71(\pm 0.01)\times 10^{-6}$ day year^{-1}, which could be attributed to mass transfer from the more massive component to the less massive one. The light-travel time effect signifies periodic oscillations, characterized by an amplitude of $A_3 = 0.0032(\pm 0.0002)$ days, and a period of $P_3 = 1.413(\pm 0.001)$ yr. $(O-C)_2$ represents the values after the parabolic trend has been removed, as detailed in Table 2 and illustrated in the middle part of Figure 2. The final residuals, obtained by applying epoch formula (2) to eliminate all trends, are documented in Table 2 and displayed in the lower part of Figure 2.

4. W-D Program Photometric Analysis

V0405 Dra has not been subjected to a published analysis of its light curve. Therefore, we have decided to conduct a detailed study of V0405 Dra. Given the consistent symmetry and stability of V0405 Dra's light curves throughout the TESS observation period, we randomly selected a sector for photometric analysis and the phased light curves are depicted in

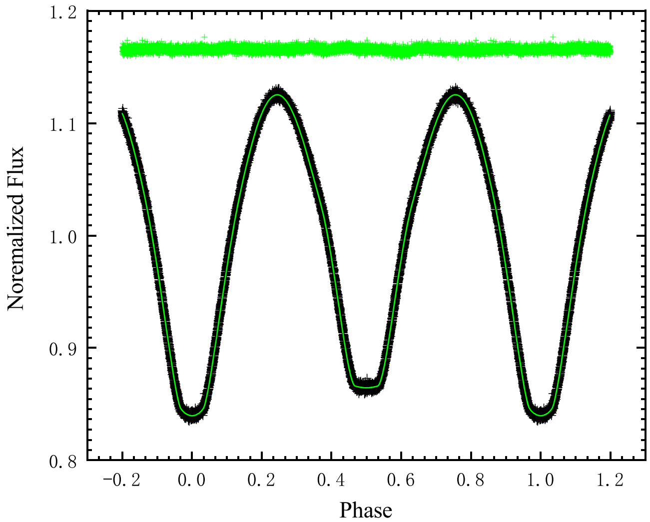

Figure 3. The comparisons between the observed and computed light curve.

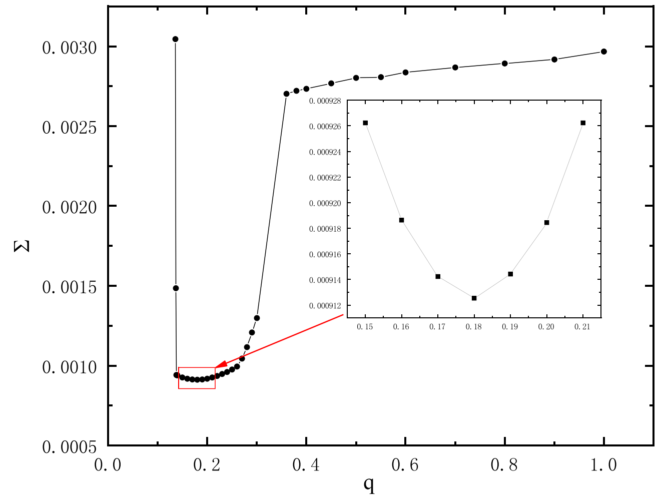

Figure 4. The $\Sigma \mathrm{res}^2 - q$ curve for V0405 Dra.

Table 3
Orbital Parameters of Light-travel Time Effect for V0405 Dra

Parameter	V0405 Dra
T(BJD)	2458683.676937(115)
$P(d)$	0.413059211(198)
$Q(\times 10^{-9} d)$	−1.532(2)
$A(d)$	0.0032(2)
e	0.085(1)
T_s(BJD)	2487333.68289(236.81513)
ω (arc)	−0.0183(54)
P_{mod}(yr)	1.413(1)
$a_{12} sini(AU)$	0.56(3)
$f(m)(M_\odot)$	0.087(1)
$M_3(i_3 = 90°)(M_\odot)$	0.78(5)
$M_3(i_3 = 60°)(M_\odot)$	0.92(1)
$M_3(i_3 = 30°)(M_\odot)$	1.93(2)

Figure 3. To model the light curve of V0405 Dra, we employed the 2013 version of the Wilson-Devinney (W-D) code (Wilson & Devinney 1971; Wilson 1979, 1990; Van Hamme & Wilson 2007; Wilson 2008; Wilson et al. 2010; Wilson 2012). We gratefully acknowledge Professor Van Hamme, one of the authors of the W-D program, for kindly providing us with the band files of TESS. Preliminary configuration of specific parameters was essential before executing the program. Initially, we established the temperature of the primary star (star 1) based on the Gaia[7] mission in Gaia Data Release 3 (DR3), setting it at $T_1 = 6685$ K, which closely approximates the provided value of 6684.603 K (Gaia Collaboration et al. 2016, 2023). We assumed the gravity darkening exponents $g_1 = g_2 = 0.32$ (Lucy 1967) and set the bolometric albedo coefficients at $A_1 = A_2 = 0.50$ (Rucinski 1973). The bolometric and bandpass limb-darkening coefficients are obtained via internal computation with the logarithmic law based on the results of van Hamme (1993). We conducted separate fits using different models: Model 1 representing an overcontact binary with multiple parameter constraints, Model 2 as detached binary, Model 3 as an overcontact binary with fewer parameter constraints, Model 4 as a semi-detached binary where star 1 accurately fills its limiting lobe, and Model 5 as a semi-detached model where star 2 fills its limiting lobe. Ultimately, only Model 3 yielded convergent results.

In the absence of previously published photometric and spectroscopic solutions for V0405 Dra, we employed a q-search method to ascertain the mass ratio. The adjustable parameters included the orbital inclination (i), the mean temperature of star 2 (T_2), the monochromatic luminosity of star 1 (L_1), and the dimensionless potential ($\Omega_1 = \Omega_2$ for model 3). We searched for photometric solutions across mass ratios from 0.1 to 1.0, establishing increments at 0.1 intervals. The process identified a minimum in the sum of squared residuals ($\Sigma \mathrm{res}^2$) at $q = 0.2$. To refine this, we narrowed the q values between 0.1 and 0.3, incrementing by 0.01, and pinpointed the minimum $\Sigma \mathrm{res}^2$ at $q = 0.18$. We then graphed the convergent solutions mapping q to $\Sigma \mathrm{res}^2$ in Figure 4, and selected $q = 0.18$ as the initial value for further adjustments to derive the final photometric solutions, which are compiled in Table 4. The orbital period analysis in Section 3 suggested cyclic changes potentially indicative of a third body, leading us to incorporate a third light (L_3) in our photometric model. The analysis determined the third light's contribution to total luminosity at 16.44(±0.14)%. The geometric configuration at phase 0.25 is depicted in Figure 5.

[7] https://gea.esac.esa.int/archive/

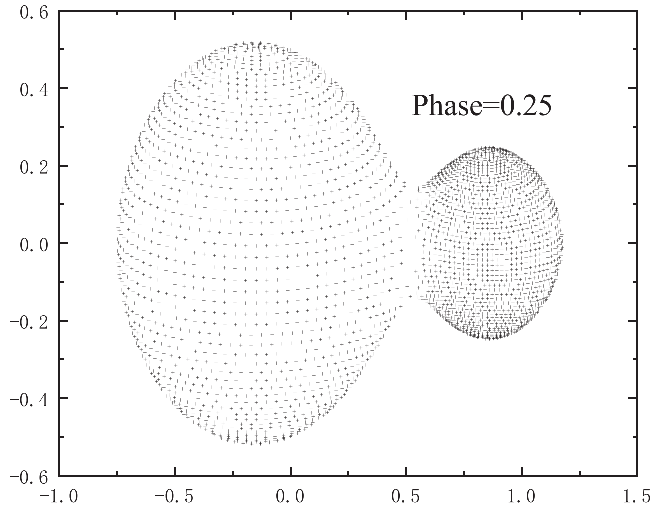

Figure 5. 0.25 phase diagram of V0405 Dra.

Table 4
Photometric Solutions for V0405 Dra

Parameter	Value	Error
Mode	3	…
$i[°]$	78.82	0.04
$q[m_2/m_1]$	0.175	0.001
$T_1[K]$	6685	Fixed
$T_2[K]$	6485	±2
$\Omega_1 = \Omega_2$	2.0913	±0.0008
$L_1/(L_1 + L_2)$	0.8274	±0.0004
$L_2/(L_1 + L_2)$	0.1726	±0.0004
$L_3/(L_1 + L_2 + L_3)$	0.1644	±0.0014
r_1(pole)	0.5168	±0.0002
r_1(side)	0.5724	±0.0002
r_1(back)	0.6004	±0.0002
r_2(pole)	0.2463	±0.0010
r_2(side)	0.2597	±0.0012
r_2(back)	0.3243	±0.0040
The degree of contact(f)	68.7%	±0.7%
Σres^2	0.000 845 47	…

5. Discussion and Conclusions

Utilizing TESS data, we performed a detailed photometric analysis of V0405 Dra using the W-D program. The analysis concludes that V0405 Dra is an A-subtype deep contact binary system, characterized by a fill-out factor of $f = 68.7(\pm0.7)\%$ and a notably small mass ratio of $q = 0.175(\pm0.001)$. The determined orbital inclination of the system is $i = 78.82°$ $(\pm0.04°)$. The symmetry and stability of V0405 Dra's light curves, especially the flat-bottomed minima, lend high reliability to these photometric solutions, aligning with the precedents and methodologies referenced in prior studies (Pribulla et al. 2003; Terrell & Wilson 2005; Zhang et al. 2017; Li et al. 2021). Despite the significant differences in mass and radius between the two stars, the temperature disparity is modest, with the more massive component being only about 200 K hotter. This small temperature difference suggests that V0405 Dra is not only in geometric contact but also in thermal equilibrium. Additionally, the detection of light contribution (L_3) potentially from a tertiary star aligns with the light-travel time effects discussed in Section 3, indicating the likely presence of a third body.

In our analysis of V0405 Dra's orbital period variations, we obtain not only a periodic variation characterized by an amplitude of $A_3 = 0.0032(\pm0.0002)$ days and a period of $P_3 = 1.413(\pm0.001)$ yr, but also a discernible long-term decrease in the orbital period at a rate of $dP/dt = -2.71(\pm0.01) \times 10^{-6}$ day year^{-1}. Referencing Allen's table (Cox & Pilachowski 2000), we estimate the primary star's spectral type as F5 and deduce its mass to be $M_1 = 1.4M_\odot$ (Cox 2000). Correspondingly, with the mass ratio $q = 0.175$, the mass of the secondary is calculated as $M_2 = 0.24M_\odot$. The consistent symmetry and stability of the light curves support the hypothesis that the detected oscillation is attributable to the light-travel time effect induced by an additional body (Irwin 1952), reinforcing the triple-system scenario posited for V0405 Dra. Using the following known formula (3),

$$f(m) = \frac{4\pi^2}{GP_3^2} \times (a_{12} sini)^3 = \frac{(M_3 sini)^3}{(M_1 + M_2 + M_3)^2}, \quad (3)$$

the mass function ($f(m)$) and the mass of the third body (M_3), assuming orbital inclination of $i_3 = 30°$, $60°$, $90°$, have been computed and are presented in Table 3. The minimum mass for the third body has been established as $M_3 = 0.78(5)M_\odot$, indicating that the third body's separation from the central binary should be less than 1.18(2) au. Thus, V0405 Dra is a new target with a quite close-in companion star, and its formation and evolution may be strongly affected by the companion star (Tokovinin et al. 2006; Zhou et al. 2017).

Regarding the period change rate, V0405 Dra manifests a decrease at $dP/dt = -2.71(\pm0.01) \times 10^{-6}$ day year^{-1}, a rate notably more pronounced than those observed in other DLMRCBs. Given the system's deep contact nature, such long-term decrease in the period could be attributed to mass transfer from the more massive component to the less massive one. Under the assumption of conservative mass transfer, by considering the conservative mass transfer equation from M_1 to M_2 (Singh & Chaubey 1986)

$$\frac{\dot{P}}{P} = 3\dot{M}_2\left(\frac{1}{M_1} - \frac{1}{M_2}\right), \quad (4)$$

the rate of mass transfer for V0405 Dra is determined to be $dM_2/dt = -6.27(\pm0.06) \times 10^{-7}M_\odot$ year^{-1}. This rate is significantly higher compared to other DLMRCBs (Li et al. 2022; Meng et al. 2023), suggesting that the fast decreases in the orbital period might result from a combination of mass transfer and angular momentum loss due to the tertiary body. Given the accelerated period decrease, V0405 Dra is likely to evolve toward a more closely contracted configuration, potentially culminating as an FK Com-type star. Stellar mergers, particularly among DLMRCBs, are anticipated outcomes in stellar evolution (Hut 1980; Rasio 1995; Kochanek et al. 2014; Yang & Qian 2015), though empirical instances such as the merger of V1309 Sco in 2008 underscore the complexity and rarity of such events (Tylenda et al. 2011; Zhu et al. 2016). The ongoing observation and study of DLMRCBs like V0405 Dra are crucial for advancing our understanding of these dynamic stellar systems.

Acknowledgments

This research was supported by the Joint Research Fund in Astronomy (grant No. U1631108) under a cooperative agreement between the National Natural Science Foundation of China (NSFC) and the Chinese Academy of Sciences (CAS), and the Chinese National Natural Science Foundation of China (NSFC, grant No. 12103030). This paper has made use of data collected by the Transiting Exoplanet Survey Satellite (TESS) mission, for which funding is provided by the NASA Explorer Program. We sincerely thank the TESS project for releasing high-precision continuous photometric data.

ORCID iDs

Lin-Qiao Jiang https://orcid.org/https://orcid.org/0000-0002-2760-8492
Jie Zheng https://orcid.org/0000-0001-6637-6973

References

Akerlof, C., Amrose, S., Balsano, R., et al. 2000, AJ, 119, 1901
Applegate, J. H. 1992, ApJ, 385, 621
Binnendijk, L. 1970, VA, 12, 217
Cox, A. N., & Pilachowski, C. A. 2000, PhT, 53, 77
Cox, A. N. (ed.), 2000, Allen's Astrophysical Quantities (New York: AIP Press)
Duchêne, G., & Kraus, A. 2013, ARA&A, 51, 269
Gaia Collaboration, Prusti, T., de Bruijne, J. H. J., et al. 2016, A&A, 595, A1
Gaia Collaboration, Vallenari, A., Brown, A. G. A., et al. 2023, A&A, 674, A1
Geske, M. T., Gettel, S. J., & McKay, T. A. 2006, AJ, 131, 633
Hut, P. 1980, A&A, 92, 167
Irwin, J. B. 1952, ApJ, 116, 211
Kochanek, C. S., Adams, S. M., & Belczynski, K. 2014, MNRAS, 443, 1319
Kopal, Z. 1955, AnAp, 18, 379
Kopal, Z. 1978, in Dynamics of Close Binary Systems, ed. Kopal (Berlin: Springer)
Kreiner, J. M., Kim, C.-H., & Nha, I.-S. 2001, An Atlas of O-C Diagrams of Eclipsing Binary Stars (Krakow: Wydawnictwo Naukowe AP)
Li, K., Gao, X., Liu, X.-Y., et al. 2022, AJ, 164, 202
Li, K., Xia, Q.-Q., Kim, C.-H., et al. 2021, AJ, 162, 13
Li, L., & Zhang, F. 2006, NewA, 11, 588
Lightkurve Collaboration, Cardoso, J. V. D. M., Hedges, C., et al. 2018, Lightkurve: Kepler and TESS time series analysis in Python, Astrophysics Source Code Library, ascl:1812.013
Lucy, L. B. 1967, ZA, 65, 89
Meng, F., Zhu, L., Qian, S., et al. 2023, ApJ, 954, 111
Pribulla, T., Kreiner, J. M., & Tremko, J. 2003, CoSka, 33, 38
Pyatnytskyy, M. Y., & Andronov, I. L. 2022, RNAAS, 6, 149
Qian, S. B., Yang, Y., Zhu, L., He, J., & Yuan, J. 2006, Ap&SS, 304, 25
Qian, S. B., Yang, Y. G., Soonthornthum, B., et al. 2005, AJ, 130, 224
Qian, S.-B., Zhu, L.-Y., Liu, L., et al. 2020, RAA, 20, 163
Rasio, F. A. 1995, ApJL, 444, L41
Ricker, G. R., Winn, J. N., Vanderspek, R., et al. 2015, JATIS, 1, 014003
Rucinski, S. 1973, PoAst, 21, 189
Sarotsakulchai, T., Qian, S. B., Soonthornthum, B., et al. 2018, AJ, 156, 199
Singh, M., & Chaubey, U. S. 1986, Ap&SS, 124, 389
Stepien, K. 2006, AcA, 56, 199
Terrell, D., Gross, J., & Cooney, W. R. 2012, AJ, 143, 99
Terrell, D., & Wilson, R. E. 2005, Ap&SS, 296, 221
Tokovinin, A., Thomas, S., Sterzik, M., & Udry, S. 2006, A&A, 450, 681
Tylenda, R., Hajduk, M., Kamiński, T., et al. 2011, A&A, 528, A114
van Hamme, W. 1993, AJ, 106, 2096
Van Hamme, W., & Wilson, R. E. 2007, ApJ, 661, 1129
Wilson, R. E. 1979, ApJ, 234, 1054
Wilson, R. E. 1990, ApJ, 356, 613
Wilson, R. E. 2008, ApJ, 672, 575
Wilson, R. E. 2012, AJ, 144, 73
Wilson, R. E., & Devinney, E. J. 1971, ApJ, 166, 605
Wilson, R. E., Van Hamme, W., & Terrell, D. 2010, ApJ, 723, 1469
Yang, Y.-G. 2009, Sci. China Ser. G-Phys., Mech. Astron., 39, 637, (in Chinese)
Yang, Y.-G., & Qian, S.-B. 2015, AJ, 150, 69
Yang, Y.-G., Wang, S., Yuan, H.-Y., & Dai, H.-G. 2021, RAA, 21, 290
Yuan, J., & Qian, S. 2007, ApJ, 669, L93
Zhang, J., Qian, S.-B., Han, Z.-T., & Wu, Y. 2017, MNRAS, 466, 1118
Zhou, X., Qian, S., & Zhang, B. 2017, PASJ, 69, 37
Zhou, X., Qian, S. B., Zhang, J., et al. 2016, ApJ, 817, 133
Zhou, X., & Soonthornthum, B. 2019, PASJ, 71, 39
Zhu, L. Y., Qian, S. B., Soonthornthum, B., He, J. J., & Liu, L. 2011, AJ, 142, 124
Zhu, L.-Y., Zhao, E.-G., & Zhou, X. 2016, RAA, 16, 68